
This is an electronic reprint of the original article.
This reprint may differ from the original in pagination and typographic detail.

Karlqvist, Susanna; Burdun, Iuliia; Salko, Sini Selina; Juola, Jussi; Rautiainen, Miina
Retrieval of moisture content of common Sphagnum peat moss species from hyperspectral and multispectral data

Published in:
Remote Sensing of Environment

DOI:
[10.1016/j.rse.2024.114415](https://doi.org/10.1016/j.rse.2024.114415)

Published: 15/12/2024

Document Version
Publisher's PDF, also known as Version of record

Published under the following license:
CC BY

Please cite the original version:
Karlqvist, S., Burdun, I., Salko, S. S., Juola, J., & Rautiainen, M. (2024). Retrieval of moisture content of common Sphagnum peat moss species from hyperspectral and multispectral data. *Remote Sensing of Environment*, 315, Article 114415. <https://doi.org/10.1016/j.rse.2024.114415>

This material is protected by copyright and other intellectual property rights, and duplication or sale of all or part of any of the repository collections is not permitted, except that material may be duplicated by you for your research use or educational purposes in electronic or print form. You must obtain permission for any other use. Electronic or print copies may not be offered, whether for sale or otherwise to anyone who is not an authorised user.



Retrieval of moisture content of common *Sphagnum* peat moss species from hyperspectral and multispectral data

Susanna Karlqvist^{*}, Iuliia Burdun, Sini-Selina Salko, Jussi Juola, Miina Rautiainen

School of Engineering, Aalto University, P.O. Box 14100, FI-00076 AALTO, Finland

ARTICLE INFO

Edited by Marie Weiss

Keywords:

Peatland
Hyperspectral
Multispectral
Spectral index
Optical trapezoid model (OPTRAM)
Continuous wavelet transform (CWT)

ABSTRACT

Peatlands store enormous amounts of carbon in a peat layer, the formation and preservation of which can only occur under waterlogged conditions. Monitoring peatland moisture conditions is critically important because a decrease in moisture leads to peat oxidation and the release of accumulated carbon back into the atmosphere as a greenhouse gas. Optical remote sensing enables the indirect monitoring of peatland moisture conditions by identifying moisture-driven changes in vegetation spectral signatures. The vegetation of northern peatlands is dominated by *Sphagnum* mosses, whose spectral signatures are known to be highly sensitive to changes in moisture content. In this study, we tested methods to estimate *Sphagnum* moisture content from spectral data using seven spectral moisture indices, the Optical TRapezoid Model (OPTRAM) and the Continuous Wavelet Transform (CWT). This study was based on data representing nine *Sphagnum* species sampled from two habitats in southern boreal peatlands in Finland. Our results showed that both multi- and hyperspectral data can be used to estimate the moisture content of *Sphagnum* mosses. Nevertheless, the optimal retrieval method depended on habitat characteristics. Using hyperspectral data, we found that: (i) the CWT exhibited superior performance for all studied moss species ($R^2_{\text{Marg}} = 0.72$, $\text{ICC} = 0.40$), (ii) the exponential OPTRAM performed best for the mesotrophic species ($R^2_{\text{Marg}} = 0.70$, $\text{ICC} = 0.08$), and (iii) the Modified Moisture Stress Index (MMSI) yielded the best results ($R^2_{\text{Marg}} = 0.68$, $\text{ICC} = 0.55$) for the ombrotrophic species. Furthermore, we demonstrated that using multispectral data instead of hyperspectral data provides comparable results in moisture estimation when used as input with OPTRAM or Moisture Stress Index (MSI). This approach could lead to new insights into the moisture dynamics in *Sphagnum*-dominated peatlands over the span of the multispectral satellite era.

1. Introduction

Peatlands, covering 3.8 % of the Earth's landmass (UNEP, 2022), are terrestrial wetland ecosystems that function as crucial carbon sinks (Limpens et al., 2008). Predominantly located in northern latitudes (Harenda et al., 2018), these unique ecosystems support rich biodiversity and play a pivotal role in the global carbon cycle (Rydin and Jeglum, 2006). The carbon stock accumulated in northern peatlands alone, ranging from 474 to 621 gigatons (Gt) of carbon (Yu et al., 2010), surpasses that of the global live forest biomass (Pan et al., 2011) and constitutes nearly one-third of the world's entire soil carbon stock (Harenda et al., 2018). This substantial carbon stock is stored within a layer of partly decomposed plant remnants known as the peat layer. In northern peatlands, the peat layer is mainly formed by *Sphagnum* peat mosses (Rydin and Jeglum, 2006).

Sphagnum peat mosses, key contributors to peatland biomass and carbon sequestration (Verhoeven and Liefveld, 1997), are highly dependent on water availability (Rydin and Jeglum, 2006). The optimal moisture content in *Sphagnum* species has been recorded to increase the CO₂ assimilation rate (Robroek et al., 2009) and mitigate the CH₄ emissions into the atmosphere (Larmola et al., 2010), resulting in a long-term climate cooling effect. However, climate warming in northern latitudes leads to shifts in northern peatland behavior due to changes in temperature and precipitation trends (Zhang et al., 2022). These trends may negatively impact the functioning of *Sphagnum* mosses and transform peatlands from carbon sinks to sources. Consequently, monitoring the moisture content of *Sphagnum* mosses can provide invaluable insights into peatland conditions and their carbon sink functions.

Conventional field methods for measuring *Sphagnum* and peatland moisture, such as manual sampling and ground-based sensors, are labor-

^{*} Corresponding author.

E-mail address: susanna.karlqvist@aalto.fi (S. Karlqvist).

<https://doi.org/10.1016/j.rse.2024.114415>

Received 21 December 2023; Received in revised form 3 September 2024; Accepted 5 September 2024

Available online 11 September 2024

0034-4257/© 2024 The Authors. Published by Elsevier Inc. This is an open access article under the CC BY license (<http://creativecommons.org/licenses/by/4.0/>).

intensive and time-consuming. Moreover, these measurements are often confined to small spatial scales, posing challenges in extrapolating findings to broader regions and potentially leading to unrealistic estimates of peatland hydrology (Harris and Bryant, 2009). In contrast, satellite remote sensing allows coverage of vast and remote areas, nearly regular resampling intervals, and cost-effective use of openly accessible data (Lees et al., 2018). Particularly, optical remote sensing enables indirect monitoring of peatland moisture conditions by identifying moisture-driven changes in vegetation spectral signatures over extensive areas (Nelson et al., 2022; Burdun et al., 2023; Olthof and Fraser, 2024).

Various methods exist to estimate moisture content of *Sphagnum* mosses from optical remote sensing data. Spectral moisture indices, utilizing shortwave infrared (SWIR) and near-infrared (NIR) bands, such as those employed by Harris et al. (2005), Letendre et al. (2008), Meingast et al. (2014) and Lees et al. (2020), have demonstrated broad and effective applicability both in laboratory settings and within *Sphagnum*-dominated peatlands. While these studies have established a robust relationship between spectral moisture indices and *Sphagnum* moisture content, their scope has often been limited, typically ranging from only two to four species. Furthermore, many of these studies have underscored the species-specific nature of the relationship between spectral indices and *Sphagnum* moisture. This specificity can complicate moisture estimation across heterogeneous peatland areas where numerous *Sphagnum* species coexist.

Sphagnum species found in the same peatland habitats often exhibit similar physiological behavior (Larmola et al., 2010), which suggests that incorporating the habitat type into the moisture estimation could potentially yield less species-dependent results (Harris et al., 2005). This hypothesis is further supported by Salko et al. (2023a), who studied nine distinct *Sphagnum* species and observed that the species from a particular habitat exhibit similar changes in the NIR and SWIR regions during desiccation. Incorporating *Sphagnum* habitat type into the moisture estimation holds promise. Although current satellite remote sensing data may not be tailored to distinguish individual species, they can still facilitate the identification of peatland habitats to a certain extent (Bourgeau-Chavez et al., 2017).

As an alternative to spectral indices, the Optical TRapezoid Model (OPTRAM) has been utilized to address the problem of species-specific relationships with moisture in peatlands, some of which had *Sphagnum* cover (Burdun et al., 2020a, 2020b; Räsänen et al., 2022; Burdun et al., 2023). Nevertheless, Burdun et al. (2023) found that the relationship between moisture and OPTRAM may be unstable over time and change under dry conditions in *Sphagnum*-dominated peatlands. Another alternative moisture estimation method is the Continuous Wavelet Transform (CWT) (Banskota et al., 2017), which outperformed two NIR-based moisture indices in a mixed-species composition experiment. However, this study only tested CWT with oligo- and ombrotrophic peatland species, including just four *Sphagnum* species.

Overall, these studies highlight the need to identify the most robust method for monitoring moisture content in various *Sphagnum* mosses with optical remote sensing. So far, only a few studies have compared classical SWIR- and NIR-based moisture indices with the more advanced OPTRAM (Räsänen et al., 2022) and CWT (Banskota et al., 2017) approaches. Moreover, most studies estimating moisture content in *Sphagnum* mosses have been carried out using only hyperspectral data (Harris et al., 2005; Van Gaalen et al., 2007; Letendre et al., 2008). Therefore, there is limited knowledge of whether multispectral data can provide equally strong results relative to hyperspectral data (Meingast et al., 2014; Lees et al., 2020). Additionally, much uncertainty remains about the relationship between moisture content and moisture indices, OPTRAM, and CWT for different *Sphagnum* species and their habitat groups.

In this paper, we present a comparison of methods for estimating boreal *Sphagnum* moss moisture content from hyperspectral and multispectral data with, to our knowledge, the largest open spectral library of *Sphagnum* species measured to date. We compared seven SWIR- and NIR-based moisture indices with more advanced methods, OPTRAM and

CWT, for monitoring moisture content in nine *Sphagnum* moss species using hyperspectral data. To assess the potential of multispectral satellite sensors for monitoring peatland moisture, we also evaluated the performance of the Moisture Stress Index (MSI) and the OPTRAM using multispectral data. Specifically, we investigated: (i) which method is the most accurate for estimating *Sphagnum* moisture content from hyperspectral data? and (ii) how do the results obtained from hyperspectral data analysis compare to those derived from multispectral data?

2. Material and methods

Our research methodology, illustrated in Fig. 1, encompasses several key steps to estimate *Sphagnum* moisture from optical data. Initially, we employed hyperspectral data (section 2.1) to calculate seven moisture indices (section 2.2), along with linear and exponential OPTRAMs (section 2.3), and CWT (section 2.4). Furthermore, we transformed the narrowband hyperspectral data into broadband data (section 2.5), enabling the calculation of multispectral estimation methods. Ultimately, we assessed the relationships between these methods and the laboratory-measured moisture content (section 2.6).

2.1. Data

We employed a publicly available spectral library of *Sphagnum* mosses assembled by Salko et al. (2023b). This dataset encompasses samples from nine *Sphagnum* species collected from four undrained and protected peatland sites in Southern Finland: Luutasuo (60.680°N, 24.321°E), Matkunsuo (60.531°N, 24.710°E), Ritasaarensuo (60.640°N, 24.962°E) and Slättmossen (60.131°N, 24.365°E). The elevations of these sites ranged from 40 to 140 m above sea level. Three species in the dataset were collected from tree fen and spruce mire habitats (*S. centrale* (C.E.O. Jensen), *S. girgensohnii* (Russow), and *S. riparium* (Ångstr.)), three from intermediate fen habitats (*S. angustifolium* (C.E.O. Jensen ex Russow) C.E.O. Jensen), *S. capillifolium* (Ehrh.) Hedw.), and *S. fallax* (H. Klinggr.) H. Klinggr.), and three from open bog habitats (*S. cuspidatum* (Ehrh. ex Hoffm.), *S. fuscum* (Schimp.) H. Klinggr.), and *S. rubellum* (Wilson)). Sampling was conducted immediately after the snowmelt in May 2022, ensuring that all samples were collected from waterlogged conditions.

For each species, ten samples measuring 21.5 × 21.7 cm were collected within either one day (*S. angustifolium*, *S. capillifolium*, *S. centrale*, *S. fallax*, *S. girgensohnii*, and *S. riparium*) or two consecutive days (*S. cuspidatum*, *S. fuscum*, *S. rubellum*). Each species was sampled from one peatland site, ensuring that the growing conditions were consistent. However, to prevent sampling from the same community, all samples were collected a minimum of 10 m apart. Each sample was extracted carefully using scissors, retaining only living plant material. The collected samples were placed in black containers, which were lidded during transportation but opened at the start of the spectral measurements and kept unlidded for the rest of the study. Additionally, the samples remained stored in the same containers to preserve their structural integrity during and between the spectral measurements. When not under measurement, the samples were left to dry in a semi-dark room, devoid of direct sunlight.

Reflectance measurements were conducted in a dark laboratory designed for spectral analysis, where the walls, doors, and ceiling were coated in black paint, and the measurement table was draped in black fabric. Each sample underwent four spectral measurements: immediately at 0 h, and after 24 h, 48 h, and 168 h (i.e., one week). These reflectance measurements were conducted with a FieldSpec-4 spectrometer (serial number: 18641) manufactured by Analytical Spectral Devices Inc. (ASD). The FieldSpec-4 covers the spectral range from 350 to 2500 nm. The measurements were acquired in nadir-view (0°), with a measurement height of 30 cm and a 25° field of view, which covers an area with a 6.7 cm radius. The samples were illuminated by a 12 V 50 W Quartz Tungsten Halogen lamp emitting a 36° beam. To minimize stray

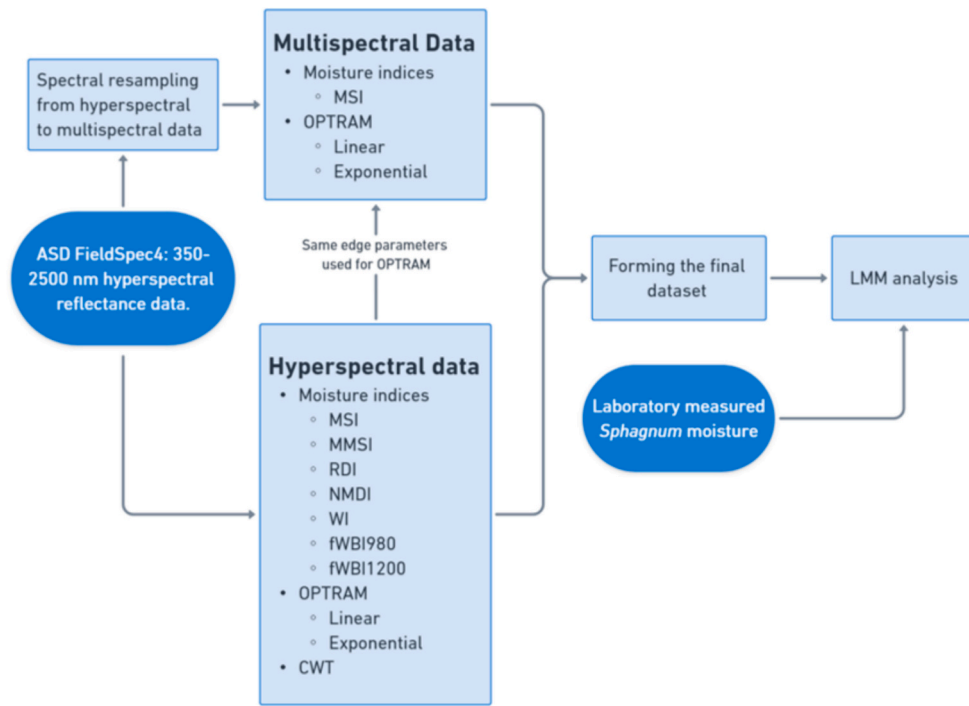


Fig. 1. Illustration of the research steps applied in the study. Dark blue indicates measured data while light blue indicates data processing or analyses. (For interpretation of the references to colour in this figure legend, the reader is referred to the web version of this article.)

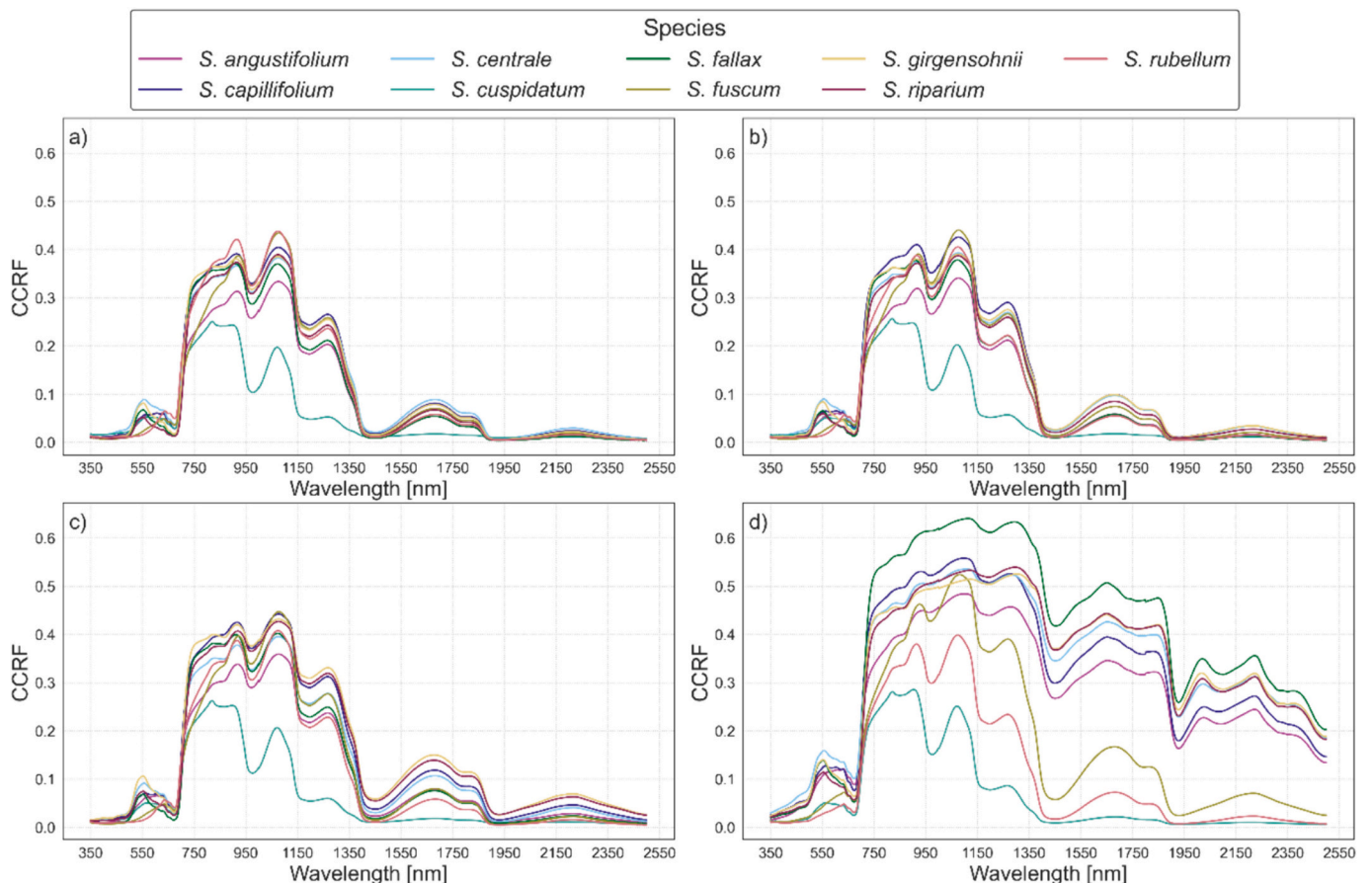


Fig. 2. Species-specific mean reflectance (conical-conical reflectance factor, CCRF) spectra of all *Sphagnum* samples at (a) 0 h, (b) 24 h, (c) 48 h, and (d) 168 h.

light, the lamp was contained within a custom-made black aluminum shade. The illumination zenith angle was set at 40°. The sample containers were positioned consistently beneath the optical fiber for each measurement, ensuring that the same area was measured each time. The measured reflectance factor was the conical-conical reflectance factor (CCRF) (Schaeppman-Strub et al., 2006). The white reference measurements used a factory-calibrated 25 × 25 cm Spectralon® panel with 99 % nominal reflectance. For a more comprehensive description of the *Sphagnum* samples and their reflectance measurements, refer to Salko et al. (2023a). The mean reflectance spectra of all samples of separate *Sphagnum* species at different measurement times are shown in Fig. 2.

Moisture estimation methods are often found to be species-specific when applied to assess *Sphagnum* moisture (Harris et al., 2005, 2006; Letendre et al., 2008; Lees et al., 2020). Therefore, to investigate whether tailoring these methods to specific habitats could enhance their performance, we categorized the *Sphagnum* species into two habitat groups based on their nutrient status. This division follows the one made by Salko et al. (2023a). The first group, termed the mesotrophic habitat group, included three species collected from nutrient-rich mesotrophic habitats: *S. centrale*, *S. girgensohnii*, and *S. riparium*, and the intermediate oligo-mesotrophic species *S. fallax*. The second group, labeled as the ombrotrophic group, comprised exclusively of the ombrotrophic species: *S. cuspidatum*, *S. fuscum*, and *S. rubellum*, alongside the intermediate ombro-minerotrophic species *S. angustifolium*. The third intermediate species, *S. capillifolium*, was excluded from the habitat division because the samples were collected from peatland ecotones.

2.2. Spectral moisture indices

We applied seven moisture indices previously used in peatland studies to estimate the *Sphagnum* moisture content (Table 1). Among the indices, two were based on the MSI originally presented by Vogelmann and Rock (1986). First, we calculated the MSI similarly to previous *Sphagnum* studies (Harris et al., 2005, 2006; Harris and Bryant, 2009; Meingast et al., 2014), which involved determining a mean reflectance value of wavelengths within specific regions for both the SWIR (1550–1750 nm) and the NIR (760–800 nm) components (Table 1). Building upon the original MSI, we introduced a modified version, termed the Modified Moisture Stress Index (MMSI) (Table 1). MMSI was inspired by the work of Arkimaa et al. (2009), who opted to utilize a maximum reflectance value for the SWIR component instead of the mean. In addition to this change, we also set the NIR component of the MMSI to its reflectance maximum.

2.3. OPTical TRApEZoid model

OPTRAM, presented by Sadeghi et al. (2017), is a surface soil moisture estimation method derived exclusively from optical data, making it suitable for applications involving optical satellite sensors such as Sentinel-2. OPTRAM is based on the premise that the distribution of observations within the STR–NDVI space correlates with the moisture content. Here, STR is the SWIR Transformed Reflectance, and NDVI is the Normalized Difference Vegetation Index. Observations with the highest STR values along the NDVI gradient are identified as the ‘wet edge’, signifying the wettest conditions, while observations with the lowest STR values along the NDVI gradient represent the ‘dry edge’, indicating the lowest moisture availability. OPTRAM can then be calculated by assuming a linear relationship between soil moisture and STR, and a linear relationship between soil moisture and vegetation moisture (Sadeghi et al., 2017) as:

$$OPTRAM = \frac{i_d + s_d \times NDVI - STR_i}{i_d - i_w + (s_d - s_w) \times NDVI} \quad (1)$$

where i_d and i_w denote the intercepts of the dry and wet edges, respectively, while s_d represents the slope of the dry edge, and s_w is the slope of

Table 1

Spectral moisture indices used in this study. The MSI equation’s “meanR” corresponds to a mean reflectance value within the specified wavelength range. In the MMSI, “maxR” represents the wavelength within the given spectral range that has the highest reflectance value. Similarly, in the case of the fWBIs and the RDI, “minR” corresponds to the wavelength with the lowest reflectance value in the provided spectral range.

Index	Equation	Reference	Previously used in peatland studies by
Moisture Stress Index (MSI)	$\frac{\text{meanR}_{1550-1750}}{\text{meanR}_{760-800}}$	Vogelmann and Rock (1986)	Harris et al. (2005, 2006); Harris and Bryant (2009); Meingast et al. (2014)
Modified Moisture Stress Index (MMSI)	$\frac{\text{maxR}_{1550-1750}}{\text{maxR}_{760-800}}$	Vogelmann and Rock (1986)	
Relative Depth Index (RDI)	$\frac{R_{1116} - \text{minR}_{1120-1250}}{R_{1116}}$	Rollin and Milton (1998)	Bryant and Baird (2003); Letendre et al. (2008)
Normalized Multiband Drought Index (NMDI)	$\frac{R_{860} - (R_{1640} - R_{2130})}{R_{860} + (R_{1640} - R_{2130})}$	Wang and Qu (2007)	Räsänen et al. (2022)
Water Index (WI)	$\frac{R_{900}}{R_{970}}$	Peñuelas et al. (1997)	Van Gaalen et al. (2007); Letendre et al. (2008); Meingast et al. (2014); Banskota et al. (2017); Salko et al. (2023a)
Floating Water Band Index (fWBI980)	$\frac{R_{920}}{\text{minR}_{960-1000}}$	Harris et al. (2005)	Harris et al. (2005, 2006); Harris and Bryant (2009); Meingast et al. (2014); Banskota et al. (2017); Lees et al. (2020)
Floating Water Band Index (fWBI1200)	$\frac{R_{920}}{\text{minR}_{1150-1220}}$	Harris et al. (2005)	Harris et al. (2005); Harris and Bryant (2009); Meingast et al. (2014)

the wet edge. STR_i represents the STR value at wavelength i and is calculated as:

$$STR = \frac{(1 - R_{SWIR})^2}{2 \times R_{SWIR}} \quad (2)$$

where R_{SWIR} represents the reflectance factor at wavelength i . OPTRAM values range from 0 (dry observations situated at the dry edge) to 1 (wet observations situated at the wet edge).

It is important to note that while OPTRAM assumes a linear relationship between soil moisture and STR, it represents merely one iteration of a broader soil moisture retrieval model outlined in Sadeghi et al. (2015), where the parameter sigma is set to one. Fixing the parameter to one simplifies soil moisture retrieval by assuming negligible scattering in saturated soils compared to dry ones. We chose to adhere to OPTRAM version of the soil moisture retrieval model due to its proven efficacy in prior peatland studies (Burdun et al., 2020a, 2020b; Räsänen et al., 2022; Burdun et al., 2023).

An alternative approach to address non-linearity in OPTRAM is with exponential OPTRAM. Introduced by Ambrosone et al. (2020) and used by Räsänen et al. (2022) in their examination of peatland moisture, exponential OPTRAM extends the linear model by incorporating exponential functions to characterize the wet and dry edges. Exponential OPTRAM is calculated as:

$$OPTRAM_{Exp} = \frac{i_d \times \exp(s_d \times NDVI) - STR_i}{i_d \times \exp(s_d \times NDVI) - i_w \times \exp(s_w \times NDVI)} \quad (3)$$

Ambrosone et al. (2020) found that exponential OPTRAM outperformed linear OPTRAM when used to study the moisture content of agricultural fields. They also observed that the exponential model was able to reduce some of the water content under and overestimation issues of the linear model. Similarly, Räsänen et al. (2022) found that exponential OPTRAM outperformed the linear model when applied separately for each peatland site.

In this study, we employed both linear and exponential OPTRAM. Furthermore, we calculated OPTRAM separately for (i) all species in the dataset, (ii) the mesotrophic species, and (iii) the ombrotrophic species.

NDVI for all OPTRAMs was calculated as:

$$NDVI = \frac{R_{NIR} - R_{Red}}{R_{NIR} + R_{Red}} \quad (4)$$

where R is the reflectance value at the chosen wavelengths in the NIR and the red regions. Although Burdun et al. (2023) discovered that the choice of vegetation index does not significantly affect OPTRAM's performance in estimating water table depth in peatlands, we assessed several wavelength pairs to calculate hyperspectral NDVI. The chosen NDVI had the strongest correlation with the moisture content and was found using the NIR wavelength 814 nm and the red wavelength 672 nm. Other tested NDVI calculations were performed using wavelengths 850 nm and 680 nm, as well as wavelengths 800 nm and 680 nm.

For calculating STR, we applied different SWIR wavelengths to the separate habitat groups (i-iii) due to their distinct relationships with the moisture content. Employing distinct values for the STR parameters enabled us to identify the optimal wavelength for computing OPTRAM within each habitat. We selected the wavelengths for the STR calculations based on the high coefficient of determination (R^2) and the low Root Mean Square Error (RMSE) values derived by fitting the STR results of different SWIR wavelengths with the laboratory-measured moisture content. Additionally, we visually evaluated the linearity and scattering between the STR and the moisture content through scatterplots (Appendix A, Fig. A1). For all species (group i), the STR was calculated from wavelength 1505 nm, the mesotrophic species (group ii) used wavelength 1375 nm, and the ombrotrophic species (group iii) wavelength 1510 nm.

Different methods exist for determining the wet and dry edge parameters. In most studies, these edges have been defined through visual inspection of NDVI–STR scatterplots (Sadeghi et al., 2017; Ambrosone et al., 2020; Burdun et al., 2020b). However, in this study, we determined the wet and dry edge parameters by optimizing the slope and intercept values of the edges to maximize the R^2 between OPTRAM and the moisture content. The parameter optimization was performed with the sequential least squares programming (SLSQP) method using the SciPy package version 1.10.1 (Virtanen et al., 2020). The initial edge parameters were set randomly, and the optimization was repeated if the final OPTRAM values fell outside the 0 to 1 range. Optimization was performed separately for all species and the two habitat groups, given their distinct STR parameters. Both linear and exponential OPTRAM underwent a similar optimization process, except that for exponential OPTRAM the initial values of both dry edge parameters were set to 0 rather than being random.

2.4. Continuous wavelet transform

CWT is an implementation of wavelet analysis that breaks down the original signal into various scales (Mallat, 1989). It was applied to analyze the moisture content of peatland plots by Banskota et al. (2017), who found that moisture content estimations were significantly improved using CWT analysis instead of spectral moisture indices. Notably, CWT also performed well with increased measurement depth.

CWT examines continuous signals across various scales through a

linear transformation of the spectrum, resulting in a series of coefficients generated using a mother wavelet function (Bruce et al., 2001). These coefficients are calculated by scaling and shifting the mother wavelet ($\psi(\lambda)$) as:

$$\psi_{a,b}(\lambda) = \frac{1}{\sqrt{a}} \psi\left(\frac{\lambda - b}{a}\right), \quad (5)$$

where components a and b represent positive real numbers, signifying the scaling and the shifting factors, respectively. We applied the second derivative of the Gaussian (DoG) function, also known as the Mexican hat, as the mother wavelet because the absorption features of vegetation spectra exhibit a Gaussian or quasi-Gaussian shape. The second DoG wavelet function is calculated as:

$$\psi(\lambda) = \frac{2}{\sqrt{3}\sqrt[4]{\pi}} \times \exp\left(-\frac{\lambda^2}{2}\right) \times (1 - \lambda^2) \quad (6)$$

Instead of using wavelet decomposition across a continuum of possible scales, we reduced the computational load by using discrete dyadic scales ($2^1, 2^2, 2^3 \dots$). We applied scales up to 2^{10} as 2^{11} was no longer informative. For ease of representation, the scales were labeled as 1, 2, 3, ..., 10.

The CWT calculation was performed using the PyWavelets package, version 1.4.1 (Lee et al., 2019). The average CWT scalogram showed the magnitude of the correlation between a portion of the reflectance spectrum and the scaled and shifted mother wavelet. This scalogram was then correlated with the laboratory-measured moisture content to assess the moisture detection performance. A correlation scalogram was calculated to display the R^2 of a simple linear regression between the moisture content and the average CWT scalogram. The CWT and the correlation scalogram calculations were performed separately for (i) all species in the dataset, (ii) the mesotrophic species, and (iii) the ombrotrophic species. The parameters, wavelength, and scale used to calculate the CWT moisture estimation indices for each of these groups were selected based on their individual correlation scalogram results.

2.5. Narrowband to broadband conversion

Following the computation of the hyperspectral moisture estimation methods, we utilized R programming language and the hsdar package (Lehner et al., 2019) to perform a narrowband to broadband conversion. The hsdar package facilitated the transformation of the hyperspectral measurements into multispectral ones by providing spectral response functions that simulate measurements obtained from a satellite sensor, in this case, specifically the thirteen spectral bands of Sentinel-2 A. Once this data transformation was completed, we proceeded to compute results for multispectral MSI and OPTRAM.

To calculate the MSI, we used Band 11 (1539–1682 nm) and Band 8 (760–907 nm). For the NDVI component of OPTRAM, we utilized Band 8 and Band 4 (646–684 nm). However, similar to the hyperspectral OPTRAM, we employed distinct bands for calculating the STR component for the separate habitat groups. For all species (group i) and the ombrotrophic species (group iii), we utilized Band 12 (2078–2320 nm), while for the mesotrophic species (group ii) we employed Band 10 (1337–1412 nm). For the OPTRAM edge parameters, we applied the same edges as with hyperspectral data (Table 3).

2.6. Statistical analyses

To assess the performance of the different estimation methods, we conducted an analysis using Linear Mixed Models (LMM). LMMs are capable of addressing correlations and dependencies within the data that arise from inherent similarities among different species. Therefore, LMMs allowed us to evaluate both the relationship between the estimation method and the moisture content, as well as the variance attributed to the species. We used R programming, with the lme4

package version 1.1.21 (Bates et al., 2015) and the performance package version 1.5.3 (Lüdtke et al., 2021) to execute and analyze the LMM results. The form of the LMM was: $\text{lmer}(\text{EstimationMethod} \sim \text{Moisture content} + (1 | \text{Species}))$. Residual plots and Q-Q plots were used to verify model assumptions. The performance of the LMM was evaluated with the conditional R^2 , the marginal R^2 (R^2_{Marg}), the intraclass correlation coefficient (ICC), and the RMSE.

Upon the initial examination of scatterplots comparing the moisture estimation methods to the moisture content, all methods, except for the CWT, displayed non-linearity and a breaking point in the data (Appendix A, Fig. A2). Beyond this breaking point, the measurements formed a flatline, indicating that the method could no longer accurately capture moisture information. Since all points beyond the breaking point corresponded to samples measured at 168 h, we restricted the LMM analysis to more linear measurements obtained within 0 to 48 h after the sample collection (Salko et al., 2023b).

3. Results and discussion

3.1. Spectral moisture indices

The performance of the seven spectral indices varied depending on the analyzed habitat group (Table 2). Overall, the best-performing spectral index was the MMSI, as it exhibited the strongest relationship with the moisture content for all species ($R^2_{\text{Marg}} = 0.73$) and the ombrotrophic species ($R^2_{\text{Marg}} = 0.68$), with lower species dependency compared to the other spectral indices. For the mesotrophic species, the MMSI's relationship ($R^2_{\text{Marg}} = 0.59$) was slightly outperformed by the RDI ($R^2_{\text{Marg}} = 0.63$). Letendre et al. (2008) also found that the RDI performed better for mesotrophic species compared to ombrotrophic ones. However, all spectral indices did exhibit species dependency, which has also been noted previously by Harris et al. (2005), Letendre et al. (2008), and Lees et al. (2020). Surprisingly, habitat division did not alleviate this dependency issue. The continuous dependency on species suggests that while species within similar habitats might share comparable physiological behavior, spectral indices might not accurately estimate moisture content of *Sphagnum* mosses without detailed species information.

Our results differed from those of Harris et al. (2005) and Meingast et al. (2014), where MSI was outperformed by other indices, most dominantly by fWBI980. The difference in results might be attributed to the wider selection of *Sphagnum* species included in our study. Specifically, the inclusion of *S. cuspidatum* could be a key factor driving these differences, as it was not considered in previous studies and exhibits a more distinct reflectance spectrum than other *Sphagnum* species (Fig. 2). Nevertheless, species that were included in both Meingast et al. (2014) and our study (*S. fuscum*, *S. angustifolium* and *S. rubellum*) did exhibit a more linear relationship with the fWBI980 than the MSI (Fig. 3). Previous studies have also noted a highly linear relationship between *Sphagnum* moisture content and the indices fWBI200 and WI (Harris et al., 2005; Van Gaalen et al., 2007). Despite our study demonstrating that the MMSI outperformed other tested moisture indices, additional studies will be needed to develop a full picture of moisture indices' performance in the field with mixed peatland species (Lees et al., 2020).

When the MSI was tested with multispectral data as input, it showed an increased relationship with the moisture for all species ($R^2_{\text{Marg}} = 0.75$), the mesotrophic species ($R^2_{\text{Marg}} = 0.61$), and the ombrotrophic species ($R^2_{\text{Marg}} = 0.71$), with decreased species dependency. The reduction in species dependency was especially notable with the ombrotrophic species, where the ICC value dropped from 0.55 to 0.39 with multispectral input data. This outcome was consistent with the results reported by Meingast et al. (2014) and Lees et al. (2020), who found that multispectral indices can give equally strong results relative to hyperspectral ones.

Table 2

Results of the LMM analysis between the moisture content and the moisture estimation methods for hyperspectral and multispectral input data for (i) all species of the dataset, (ii) the mesotrophic species, and (iii) the ombrotrophic species.

All species				
Hyperspectral input data	Conditional R2	Marginal R2	ICC	RMSE
MSI	0.91	0.71	0.70	0.03
MMSI	0.91	0.73	0.67	0.03
RDI	0.94	0.57	0.86	0.02
NMDI	0.92	0.57	0.80	0.02
WI	0.96	0.04	0.96	0.07
fWBI980	0.96	0.05	0.96	0.06
fWBI200	0.96	0.05	0.96	0.17
Linear OPTRAM	0.87	0.67	0.60	0.09
Exponential OPTRAM	0.87	0.67	0.59	0.09
CWT	0.83	0.72	0.40	0.01
Multispectral input data				
MSI	0.91	0.75	0.65	0.03
Linear OPTRAM	0.87	0.66	0.63	0.10
Exponential OPTRAM	0.87	0.66	0.62	0.10
Mesotrophic species				
Hyperspectral input data				
MSI	0.89	0.59	0.73	0.03
MMSI	0.90	0.59	0.74	0.03
RDI	0.89	0.63	0.71	0.02
NMDI	0.88	0.50	0.76	0.02
WI	0.88	0.50	0.76	0.03
fWBI980	0.88	0.53	0.74	0.02
fWBI200	0.88	0.50	0.76	0.08
Linear OPTRAM	0.82	0.62	0.52	0.08
Exponential OPTRAM	0.73	0.70	0.08	0.08
CWT	0.45	0.29	0.23	0.01
Multispectral input data				
MSI	0.89	0.61	0.72	0.03
Linear OPTRAM	0.81	0.63	0.49	0.08
Exponential OPTRAM	0.71	0.69	0.06	0.08
Ombrotrophic species				
Hyperspectral input data				
MSI	0.85	0.67	0.55	0.03
MMSI	0.86	0.68	0.55	0.03
RDI	0.94	0.34	0.91	0.02
NMDI	0.93	0.45	0.87	0.02
WI	0.96	0.03	0.99	0.10
fWBI980	0.96	0.03	0.96	0.08
fWBI200	0.96	0.03	0.96	0.24
Linear OPTRAM	0.78	0.55	0.53	0.10
Exponential OPTRAM	0.79	0.55	0.53	0.09
CWT	0.83	0.39	0.72	0.02
Multispectral input data				
MSI	0.83	0.71	0.39	0.03
Linear OPTRAM	0.78	0.51	0.56	0.12
Exponential OPTRAM	0.78	0.50	0.57	0.12

3.2. Optical TRAPezoid model

The performance of the linear and exponential OPTRAM, with the optimized edges (Table 3), yielded nearly identical results when all species were considered. The R^2_{Marg} values reflecting the relationships between both OPTRAMs and moisture content were 0.67 with hyperspectral data (Table 2). Additionally, both models exhibited high species dependency, with ICC value of 0.60 for the linear and 0.59 for the exponential model. For the mesotrophic and the ombrotrophic species, the linear OPTRAM exhibited R^2_{Marg} values of 0.62 and 0.55, respectively, while the corresponding ICC values were 0.52 and 0.53. These results suggest that categorizing species into habitat groups does not enhance the performance of the linear OPTRAM. In contrast, applying the exponential model to habitat groups resulted in great improvements for the mesotrophic species, with an R^2_{Marg} value of 0.70 and a significantly lower ICC value of 0.08, indicating minimal species dependency. This outcome is similar to the results of Räsänen et al. (2022), who reported improved performance of the exponential model over the linear

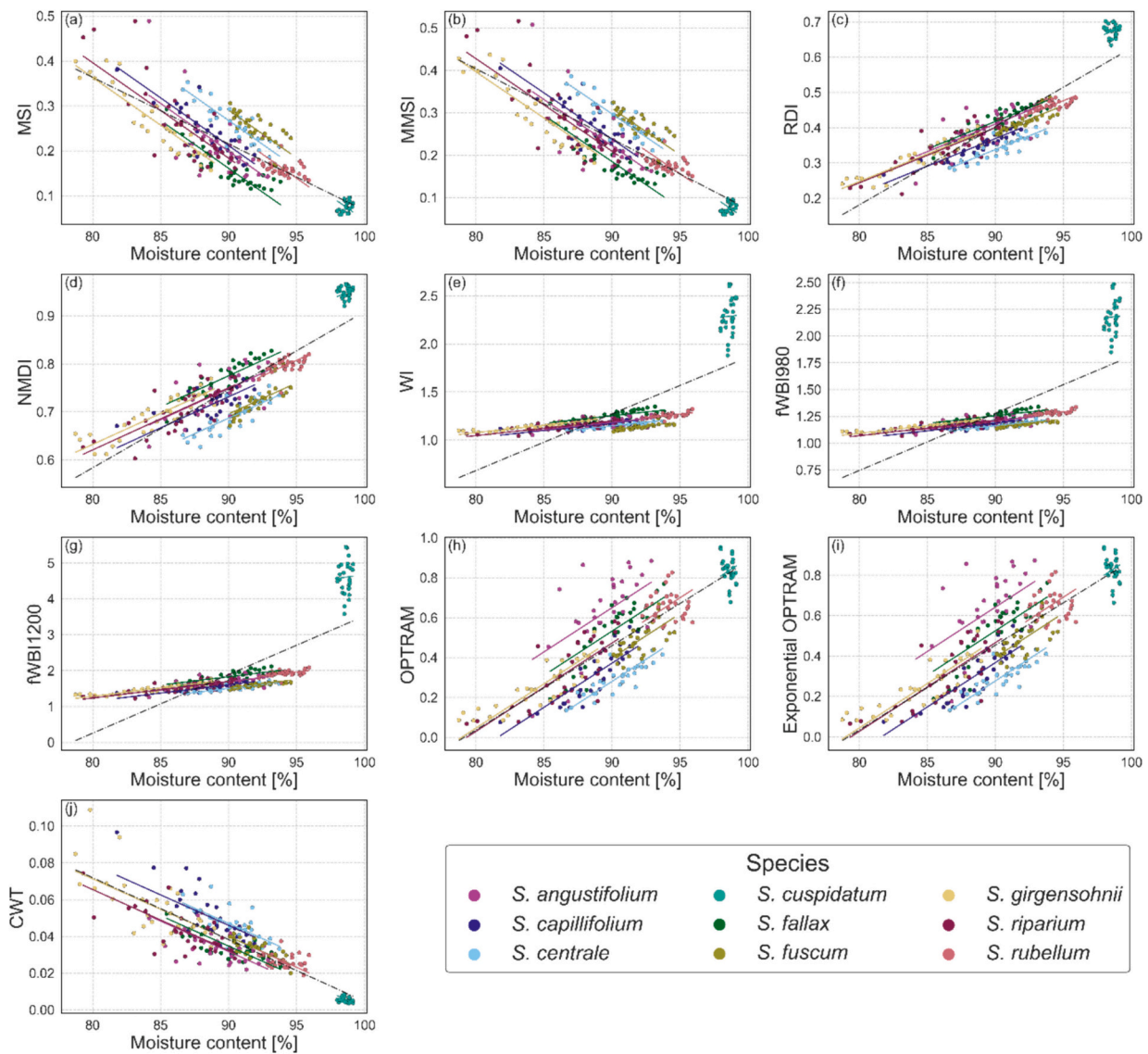


Fig. 3. The LMM regression separated by species and a simple linear regression of 0–48 h samples between the moisture content and the (a) MSI, (b) MMSI, (c) RDI, (d) NMDI, (e) WI, (f) fWBI980, (g) fWBI1200, (h) OPTRAM (i) Exponential OPTRAM, and (j) CWT.

Table 3
Optimized OPTRAM edge parameters for the linear and exponential models.

	Intercept of dry edge	Slope of dry edge	Intercept of wet edge	Slope of wet edge
Linear OPTRAM: All species	0.73	-0.99	2.97	55.51
Exponential OPTRAM: All species	0.00	0.60	19.66	1.11
Linear OPTRAM: Mesotrophic species	0.26	-0.25	0.00	8.20
Exponential OPTRAM: Mesotrophic species	0.00	2.98	0.54	3.03
Linear OPTRAM: Ombrotrophic species	0.62	0.13	26.37	25.60
Exponential OPTRAM: Ombrotrophic species	0.32	0.53	26.14	0.73

model when applied separately to each peatland habitat. For the ombrotrophic species, the exponential OPTRAM performed similarly to the linear model, producing nearly identical results (Table 2).

The analysis of multispectral data revealed findings consistent with those from the hyperspectral data. For all species, both models exhibited R^2_{Marg} value of 0.66, with ICC values of 0.63 and 0.62 for the linear and exponential models, respectively. This outcome was also true for the mesotrophic and ombrotrophic habitat groups (Table 2), suggesting that hyperspectral data may not be a prerequisite for effective peatland moisture estimation using OPTRAM models.

Our R^2_{Marg} value for the ombrotrophic *Sphagnum* species was notably lower than the R^2 reported by Burdun et al. (2023), who found a strong relationship ($R^2 = 0.8-0.9$) between OPTRAM derived from Sentinel-2 data and the water table depth in *Sphagnum*-dominated ombrotrophic peatlands. We expected similar or even stronger relationships between OPTRAM and the moisture content since moisture indices and even CWT are known to better reflect moisture content than water table depth in *Sphagnum* mosses (Harris et al., 2006; Meingast et al., 2014; Banskota et al., 2017). This discrepancy might be explained by limitations of the dataset since it did not contain observations for the period between 48 and 168 h or beyond. Within the timescale of the experiment, the

ombrotrophic species underwent desiccation to a much lesser extent than the mesotrophic species, likely due to their habitat-specific traits influencing water storage and loss. For example, *Sphagnum* species with large hyaline cells have been shown to resist desiccation and maintain higher plant water content (Rice et al., 2008). Additionally, the disparities can be attributed to the difference in spatial and temporal scales. While our study utilized small-scale laboratory data focusing on the surface moisture dynamics within a controlled environment, satellite-based studies capture large-scale data and estimate water table levels that reflect broader environmental dynamics over extended periods (Tian et al., 2020). Consequently, these differences may account for the more pronounced correlation with water-table levels identified in satellite-based studies compared to our observations of surface peat moisture.

Another important finding was that we observed a breaking point in the relationships between both OPTRAMs and the moisture content after one week of desiccation (Appendix A, Fig. A2). Similar breaking points were also observed with the spectral moisture indices, prompting the LMM analysis to exclude the 168 h measurements. Similarly, Burdun et al. (2023) reported breaking points between OPTRAM and water table depth in peatlands. These observations collectively suggest a limited moisture range for OPTRAM applicability. Therefore, future studies should exercise caution when utilizing OPTRAM under extremely dry conditions in peatlands. This limitation could potentially be addressed by adjusting the sigma parameter of OPTRAM to capture non-linear data patterns more effectively. Notably, Norouzi et al. (2022) demonstrated the effectiveness of different sigma values in moisture estimation across various soil types exhibiting non-linear trends. While this approach has not been specifically explored in the context of peatlands, it holds potential for achieving more accurate moisture estimations. However, introducing a new parameter would increase computational complexity, potentially making the model less desirable for remote sensing applications.

3.3. Continuous wavelet transform

We selected the parameters for the CWT moisture estimation indices for each habitat group based on their individual correlation scalogram results (Fig. 4). The highest R^2 value for all species ($R^2 = 0.81$) occurred at a wavelength of 1852 nm with a scale of 7. The mesotrophic species exhibited the highest R^2 ($R^2 = 0.80$) at 1138 nm with a scale of 6, while the ombrotrophic species showed the highest R^2 ($R^2 = 0.86$) at 894 nm with a scale of 5. Consequently, we chose these parameters for calculating the CWT moisture estimation indices in the LMM analyses.

The CWT coefficients obtained in this study for the ombrotrophic species exhibited similarities with coefficients obtained by Banskota et al. (2017) for their oligotrophic peatland sites. In both studies, the peak R^2 values were observed for wavelengths in the NIR region, indicating the utility of NIR wavelengths for ombro- and oligotrophic peatland sites. The NIR wavelengths have also been found to have the best relationship with moisture content and peatland vegetation in studies by Harris et al. (2005), Letendre et al. (2008), and Meingast et al. (2014). While no prior study had applied CWT to mesotrophic peatland sites, our results suggest that the NIR wavelengths also show a higher correlation with *Sphagnum* moisture than the SWIR wavelengths. However, for all species, the SWIR wavelengths exhibited a higher correlation with the moisture compared to the NIR wavelengths. Across all analyses, the highest correlations were observed at middle-frequency scales.

The results of the LMM analysis indicated that when all species were considered, the CWT had the highest R^2_{Marg} value ($= 0.72$) among hyperspectral methods and the lowest species dependency of all the methods ($\text{ICC} = 0.40$). For the mesotrophic species, the CWT exhibited even lower species dependency ($\text{ICC} = 0.23$) but was less effective in estimating the moisture content ($R^2_{\text{Marg}} = 0.29$). For the ombrotrophic species, the CWT also struggled to accurately estimate moisture content ($R^2_{\text{Marg}} = 0.39$) while simultaneously having high species dependency ($\text{ICC} = 0.72$).

Although the CWT performed well, when all the species were considered, Banskota et al. (2017) found it to outperform spectral moisture indices more significantly. Similar findings of CWT's superiority have also been reported in studies detecting the moisture content of vascular plants' leaves (Cheng et al., 2011; Li et al., 2016) and tree canopies (Cheng et al., 2014). This disparity in results and the decline of the CWT's performance with the habitat groups may be attributed to the choice of selected CWT coefficients: wavelength and scale. The coefficients were derived from the correlation scalograms generated for samples including all measurement times, while the subsequent LMM analysis focused exclusively on fresher (0 h–48 h) samples. This finding suggests that CWT results may vary based on the mean moisture levels of the studied samples. However, in addition to the peak coefficients, the CWT demonstrated high correlation results across multiple other wavelengths and scales, indicating potential performance enhancement through the exploration of more optimal coefficients or combination of coefficients. Future research should explore more comprehensive coefficient optimization, to enhance the robustness and reliability of CWT for remote sensing applications in *Sphagnum*-dominated peatlands.

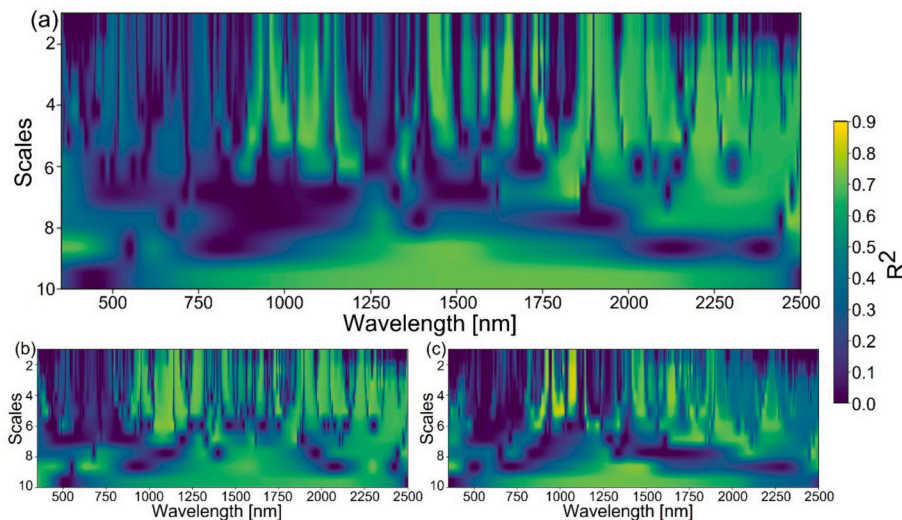


Fig. 4. The correlation scalograms for (a) all species, (b) the mesotrophic species, and (c) the ombrotrophic species, where the colour presents the R^2 between moisture content and transformed wavelet at different wavelengths and scales. The correlation scalograms were performed for the data with all observations (0 h–168 h).

3.4. Evaluation of methods from the perspective of remote sensing

All methods evaluated in this study provided varying degrees of accuracy in estimating *Sphagnum* moisture (Table 2). The spectral moisture indices, while computationally less demanding than CWT and OPTRAM, exhibited consistently high ICC values, indicating strong clustering and species variance. This result underscored the species-specific nature of spectral moisture indices, emphasizing the necessity of species knowledge for accurate moisture estimations, even with habitat divisions. In contrast, the CWT exhibited lower ICC values for the all-species group, while the exponential OPTRAM appeared uniform over the mesotrophic species.

The top-performing moisture estimation methods derived from hyperspectral data were the CWT, the OPTRAM, and the MMSI/MSI. When all species were considered, the MMSI exhibited the strongest relationship with the moisture content ($R_{\text{Marg}}^2 = 0.73$), closely followed by the CWT ($R_{\text{Marg}}^2 = 0.72$). Notably, from the perspective of practical remote sensing, the CWT also displayed significantly lower species dependency compared to the other methods, indicating a more accurate moisture estimation across different species. Additionally, the CWT had the smallest RMSE, indicating a narrow error margin. Furthermore, the CWT was the sole method to provide information from the drier *Sphagnum* samples, lacking a noticeable breaking point in the data (Appendix A, Fig. A2). This characteristic renders CWT particularly valuable for studies focusing on dry peatlands at a fine scale, such as wildfire prevention (Nelson et al., 2022), or peatland drought recovery (Lees et al., 2021). Therefore, we conclude that the CWT appeared as the most effective method across all species when hyperspectral data were available.

For both hyperspectral and multispectral data, the exponential OPTRAM excelled for the mesotrophic *Sphagnum* species, surpassing the other techniques by establishing a strong relationship with the moisture content and exhibiting a remarkably low species dependency that rendered the species factor negligible. In contrast, the MSI outperformed the exponential OPTRAM for the ombrotrophic species, exhibiting a significantly stronger relationship with the moisture content. Interestingly, the multispectral MSI outperformed its hyperspectral counterpart by displaying reduced species dependency and a stronger relationship with the moisture content.

In the experiment, the mesotrophic species demonstrated a more immediate and more intense response to desiccation (Salko et al., 2023a). Similarly, mesotrophic peatland vegetation is often more susceptible to drying compared to ombrotrophic peatland species as they are acclimated to a steadier supply of water. As such, they are more vulnerable to the warming climate (Laine et al., 2021), and retrieving data from their state of well-being is increasingly important. Overall, our results suggest that exponential OPTRAM is more effective with mesotrophic species, while MSI performs better for ombrotrophic species. This outcome implies that the selection of the monitoring method for assessing moisture content of *Sphagnum* mosses should be guided by the specific species or habitat under investigation.

This study marks the first application of the spectral region ranging from 1337 nm to 1412 nm (corresponding to, e.g., the Cirrus band of Sentinel-2 MSI) to calculate OPTRAM. Previous satellite-based peatland studies have used a wavelength range centered around 2200 nm (Burdun et al., 2020a, 2020b, 2023; Räsänen et al., 2022), while other satellite-based OPTRAM moisture studies have also applied either this band (Sadeghi et al., 2017; Huang et al., 2019; Ambrosone et al., 2020; Hassanpour et al., 2020; Das et al., 2023; Mokhtari et al., 2023) or a band centered around 1610 nm (Dubinin et al., 2020; Acharya et al., 2022; Das et al., 2023).

Based on our findings, the spectral band centered at 1375 nm holds significant promise for moisture estimation in mesotrophic peatland sites. However, it is crucial to validate this finding across a wider range of natural peatland environments before considering broader applications. Furthermore, for OPTRAM to be reliably used for peatland

moisture estimation via satellite remote sensing, future research should focus on establishing universal edge parameters that are robust across different species compositions to avoid the need for calculating edge parameters for each study.

Based on our results, the CWT method, which performed best for all *Sphagnum* species, holds great potential in light of new and future hyperspectral satellite missions (e.g., EnMAP, PRISMA, CHIME). On the other hand, results from the hyperspectral data did not surpass those from the multispectral data using OPTRAM and MSI. This result implies that multispectral satellite sensors (e.g., Sentinel-2, Landsat series) have an important role in certain peatland monitoring applications, and that hyperspectral satellite data may not be a requirement for estimating moisture content in *Sphagnum*-dominated peatlands. However, given our observation that exponential OPTRAM performs better with mesotrophic species and MSI with ombrotrophic species, recommending the use of different methods for varying habitats may pose practical challenges, given the presence of multiple habitat types within large peatland complexes (Rydin and Jeglum, 2006). Although, in the future, high spatial resolution satellite data may provide more useful aid for identifying habitat types of peatlands (Arasumani et al., 2023) and hence make it more convenient to use habitat-specific methods for peatland moisture estimation.

4. Conclusion

In this study, we assessed the applicability of hyperspectral and multispectral data for estimating *Sphagnum* moisture content using seven spectral moisture indices, OPTRAM and CWT. The dataset, encompassing nine *Sphagnum* species, enabled a comprehensive analysis of these methods, offering insights into their performance across different species and habitats. Furthermore, the results obtained here shed light on the strengths and weaknesses of each method, contributing to an understanding of their applicability in detecting *Sphagnum* moisture content. Overall, our results demonstrated that the moisture content of *Sphagnum* mosses can be estimated using both multi- and hyperspectral data. However, the most effective retrieval method depended on the habitat type. The CWT outperformed the other methods when all *Sphagnum* species were considered, but for the mesotrophic group, the exponential OPTRAM provided superior results with no species dependency, while the ombrotrophic species favored the MMSI. These results indicate that the monitoring method should be tailored to the specific habitat being studied.

The CWT method, which performed best for all species with the least species dependency, is a promising method in the context of recently launched and future hyperspectral satellite missions. However, our results additionally emphasized the potential for using multispectral satellite sensors in peatland studies, as the multispectral exponential OPTRAM and MSI could estimate the *Sphagnum* moisture for the mesotrophic and the ombrotrophic species as well as their hyperspectral counterparts with less species dependency.

CRedit authorship contribution statement

Susanna Karlqvist: Writing – original draft, Visualization, Software, Methodology, Formal analysis, Conceptualization. **Iuliia Burdun:** Writing – review & editing, Supervision, Methodology, Conceptualization. **Sini-Selina Salko:** Writing – review & editing, Investigation, Data curation. **Jussi Juola:** Writing – review & editing, Software, Investigation. **Miina Rautiainen:** Writing – review & editing, Supervision, Project administration, Methodology, Funding acquisition, Conceptualization.

Declaration of competing interest

The authors declare that they have no known competing financial interests or personal relationships that could have appeared to influence

the work reported in this paper.

Data availability

The data used in this article is available in Mendeley Data (<https://doi.org/10.17632/wm5fcdmzd.1>).

Acknowledgements

We thank Dr. Aarne Hovi for scientific collaboration in different

stages of this work. The study received funding from the Research Council of Finland (grant: PEATSPEC 3341963) and J.J. was funded by the Finnish Natural Resources Research Foundation. This study has also received funding from the European Research Council (ERC) under the European Union’s Horizon 2020 research and innovation programme (grant agreement No 771049). The text reflects only the authors’ view and the Agency is not responsible for any use that may be made of the information it contains. Finally, we thank the anonymous reviewers who improved the clarity, precision, accuracy, and relevance of this paper.

Appendix A. Appendix

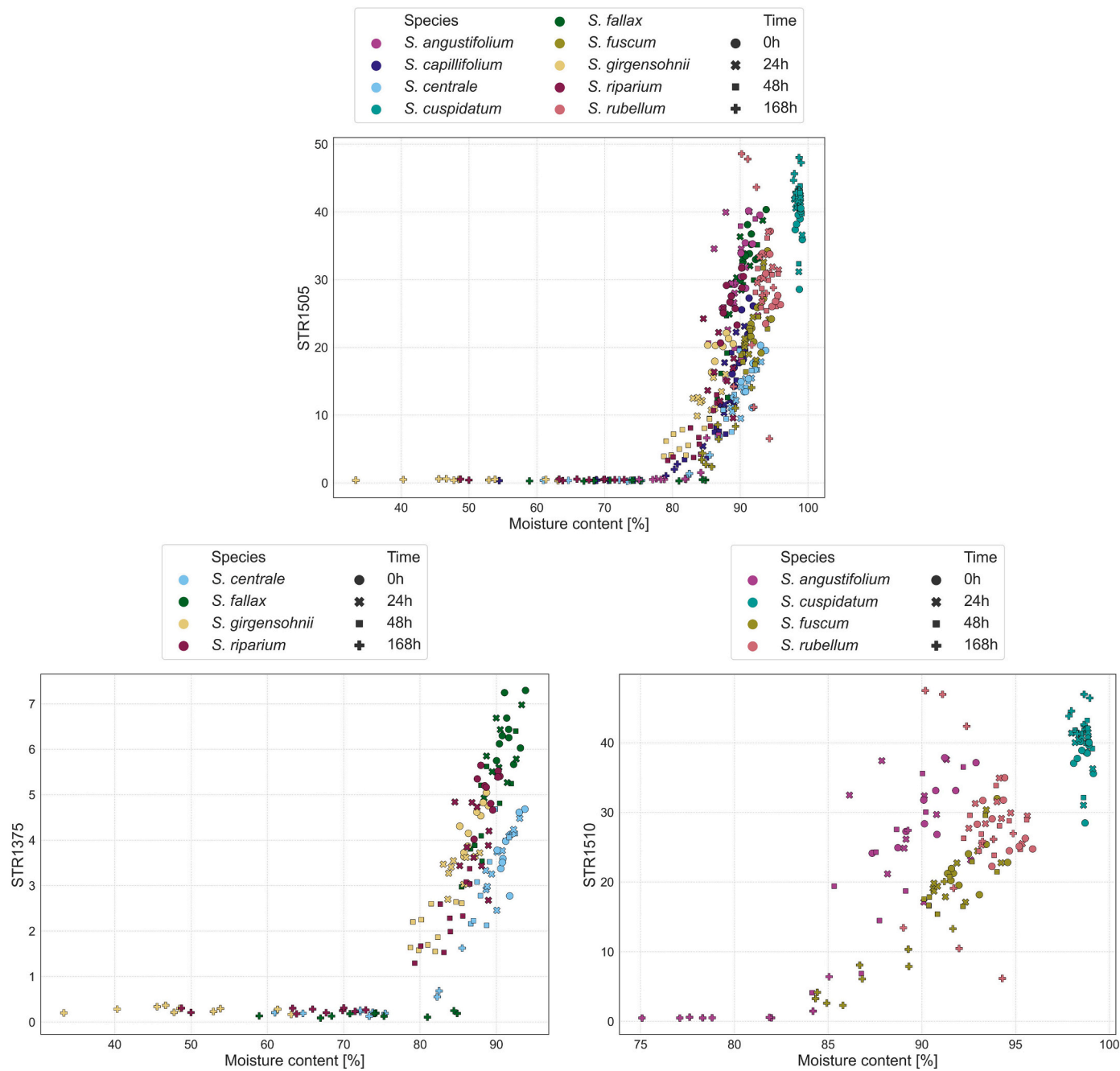


Fig. A1. Scatterplots between the moisture content and (a) STR calculated for reflectance at 1505 nm with all species, (b) STR calculated for reflectance at 1375 nm for the mesotrophic species and (c) STR calculated for reflectance at 1510 nm for the ombrotrophic species

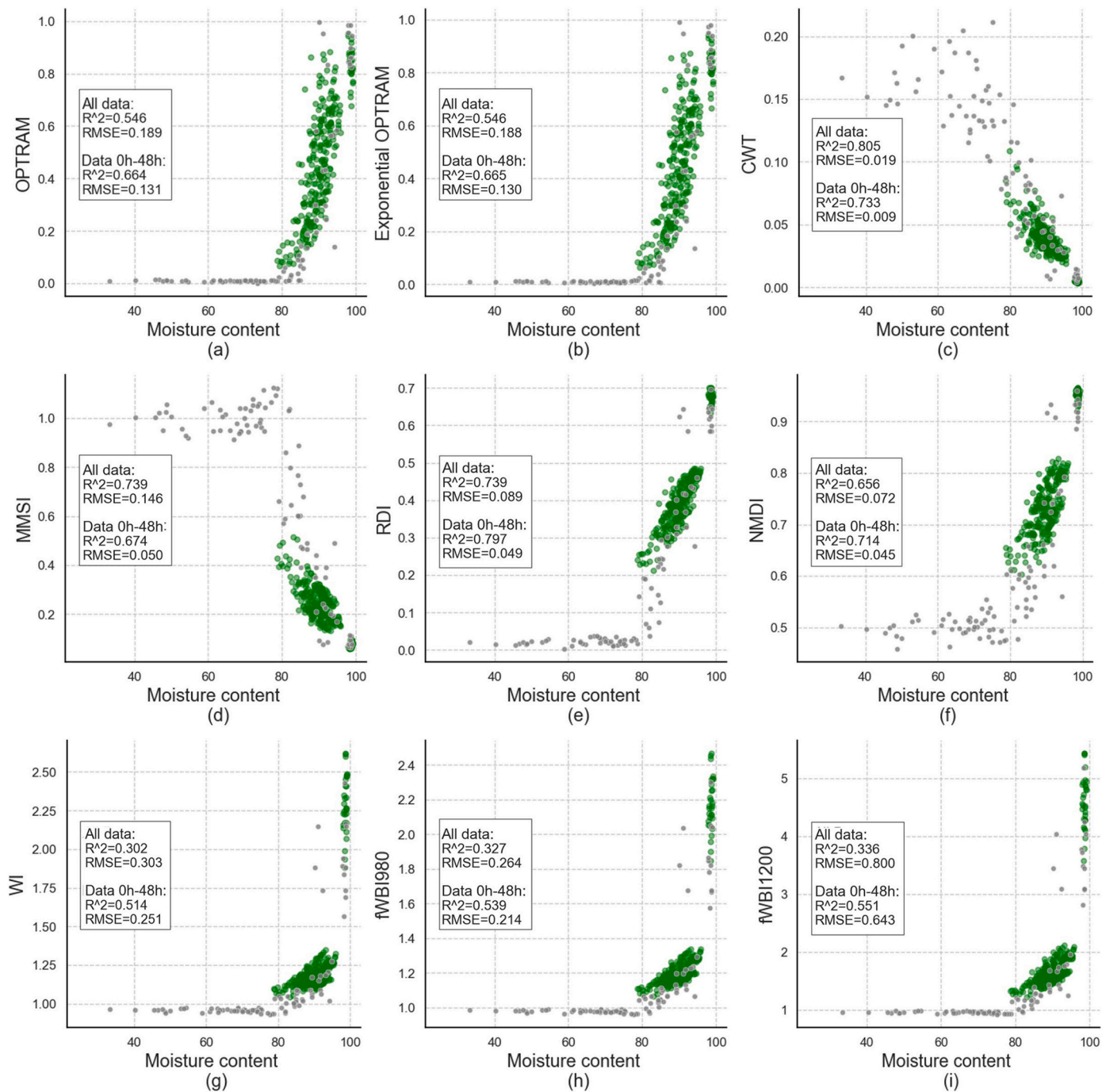


Fig. A2. Scatterplots between the moisture content and (a) OPTRAM, (b) exponential OPTRAM, (c) CWT, (d) MMSI, (e) RDI, (f) NMDI, (g) WI, (h) fWBI980 and (i) fWBI1200. Green points correspond to observation between 0 and 48 h and gray points correspond to 168 h observations. The R^2 and the RMSE values are the results of a simple linear regression. (For interpretation of the references to colour in this figure legend, the reader is referred to the web version of this article.)

References

- Acharya, U., Daigh, A.L.M., Oduor, P.G., 2022. Soil moisture mapping with moisture-related indices, OPTRAM, and an integrated random Forest-OPTRAM algorithm from Landsat 8 images. *Remote Sens.* 14 (15), 3801. <https://doi.org/10.3390/rs14153801>.
- Ambrosone, M., Matese, A., Di Gennaro, S.F., Gioli, B., Tudoroiu, M., Genesio, L., Toscano, P., et al., 2020. Retrieving soil moisture in rainfed and irrigated fields using Sentinel-2 observations and a modified OPTRAM approach. *Int. J. Appl. Earth Obs. Geoinf.* 89, 102–113. <https://doi.org/10.1016/j.jag.2020.102113>.
- Arasumani, M., Thiel, F., Pham, V.-D., Hellmann, C., Kaiser, M., van der Linden, S., 2023. Advancing peatland vegetation mapping by spaceborne imaging spectroscopy. *Ecol. Indic.* 154, 110665 <https://doi.org/10.1016/j.ecolind.2023.110665>.
- Arkimaa, H., Laitinen, J., Korhonen, R., Moisanen, M., Hirvasniemi, T., Kuosmanen, V., 2009. Spectral reflectance properties of Sphagnum moss species in Finnish mires. In: 6th EARSeL SIG IS Workshop, Imaging Spectroscopy: Innovative Tool for Scientific and Commercial Environmental Applications, pp. 16–19.
- Banskota, A., Falkowski, M.J., Smith, A.M.S., Kane, E.S., Meingast, K.M., Bourgeau-Chavez, L.L., French, N.H., et al., 2017. Continuous wavelet analysis for spectroscopic determination of subsurface moisture and water-table height in northern peatland ecosystems. *IEEE Trans. Geosci. Remote Sens.* 55 (3), 1526–1536. <https://doi.org/10.1109/tgrs.2016.2626460>.
- Bates, D., Mächler, M., Bolker, B., Walker, S., 2015. Fitting Linear Mixed-Effects Models Using lme4. *J. Stat. Software* 67 (1). <https://doi.org/10.18637/jss.v067.i01>.
- Bourgeau-Chavez, L.L., Endres, S., Powell, R., Battaglia, M.J., Benschoter, B., Turetsky, M., Banda, E., et al., 2017. Mapping boreal peatland ecosystem types from

- multitemporal radar and optical satellite imagery. *Can. J. For. Res.* 47 (4), 545–559. <https://doi.org/10.1139/cjfr-2016-0192>.
- Bruce, L.M., Morgan, C., Larsen, S., 2001. Automated detection of subpixel hyperspectral targets with continuous and discrete wavelet transforms. *IEEE Trans. Geosci. Remote Sens.* 39 (10), 2217–2226. <https://doi.org/10.1109/36.957284>.
- Bryant, R.G., Baird, A.J., 2003. The spectral behaviour of Sphagnum canopies under varying hydrological conditions. *Geophys. Res. Lett.* 30 (3) <https://doi.org/10.1029/2002GL016053>.
- Burdun, I., Bechtold, M., Sagris, V., Komisarenko, V., De Lannoy, G., Mander, Ü., 2020a. A comparison of three trapezoid models using optical and thermal satellite imagery for water table depth monitoring in Estonian bogs. *Remote Sens.* 12 (12), 1980. <https://doi.org/10.3390/rs12121980>.
- Burdun, I., Bechtold, M., Sagris, V., Lohila, A., Humphreys, E., Desai, A.R., Mander, Ü., et al., 2020b. Satellite determination of peatland water table temporal dynamics by localizing representative pixels of a SWIR-based moisture index. *Remote Sens.* 12 (18), 2936. <https://doi.org/10.3390/rs12182936>.
- Burdun, I., Bechtold, M., Aurela, M., De Lannoy, G., Desai, A.R., Humphreys, E., Rautiainen, M., et al., 2023. Hidden becomes clear: optical remote sensing of vegetation reveals water table dynamics in northern peatlands. *Remote Sens. Environ.* 296, 113736 <https://doi.org/10.1016/j.rse.2023.113736>.
- Cheng, T., Rivard, B., Sánchez-Azofeifa, A., 2011. Spectroscopic determination of leaf water content using continuous wavelet analysis. *Remote Sens. Environ.* 115 (2), 659–670. <https://doi.org/10.1016/j.rse.2010.11.001>.
- Cheng, T., Riaño, D., Ustin, S.L., 2014. Detecting diurnal and seasonal variation in canopy water content of nut tree orchards from airborne imaging spectroscopy data using continuous wavelet analysis. *Remote Sens. Environ.* 143, 39–53. <https://doi.org/10.1016/j.rse.2013.11.018>.
- Das, B., Rathore, P., Roy, D., Chakraborty, D., Bhattacharya, B.K., Mandal, D., Kumar, P., et al., 2023. Ensemble surface soil moisture estimates at farm-scale combining satellite-based optical-thermal-microwave remote sensing observations. *Agric. For. Meteorol.* 339, 109567 <https://doi.org/10.1016/j.agrformet.2023.109567>.
- Dubinina, V., Svoray, T., Stavi, I., Yizhaq, H., 2020. Using LANDSAT 8 and VENUS Data to Study the Effect of Geodiversity on Soil Moisture Dynamics in a Semiarid Shrubland. In: *Remote Sensing*, p. 3377. <https://doi.org/10.3390/rs12203377>.
- Harendra, K.M., Lamentowicz, M., Samson, M., Chojnicki, B.H., 2018. The role of peatlands and their carbon storage function in the context of climate change. In: Zieliński, T., Sagan, I., Surosz, W. (Eds.), *Interdisciplinary Approaches for Sustainable Development Goals: Economic Growth, Social Inclusion and Environmental Protection*. Springer International Publishing, Cham, pp. 169–187. https://doi.org/10.1007/978-3-319-71788-3_12.
- Harris, A., Bryant, R.G., 2009. A multi-scale remote sensing approach for monitoring northern peatland hydrology: present possibilities and future challenges. *J. Environ. Manag.* 90 (7), 2178–2188. <https://doi.org/10.1016/j.jenvman.2007.06.025>.
- Harris, A., Bryant, R.G., Baird, A.J., 2005. Detecting near-surface moisture stress in Sphagnum spp. *Remote Sens. Environ.* 97 (3), 371–381. <https://doi.org/10.1016/j.rse.2005.05.001>.
- Harris, A., Bryant, R.G., Baird, A.J., 2006. Mapping the effects of water stress on Sphagnum: preliminary observations using airborne remote sensing. *Remote Sens. Environ.* 100 (3), 363–378. <https://doi.org/10.1016/j.rse.2005.10.024>.
- Hassanpour, R., Zarehagh, D., Neyshabouri, M.R., Feizizadeh, B., Rahmati, M., 2020. Modification on optical trapezoid model for accurate estimation of soil moisture content in a maize growing field. *J. Appl. Remote. Sens.* 14 (3), 034519 <https://doi.org/10.1117/1.JRS.14.034519>.
- Huang, F., Wang, P., Ren, Y., Liu, R., 2019. Estimating Soil Moisture Using the Optical Trapezoid Model (OPTRAM) in a Semi-Arid Area of SONGNEN Plain, China Based On Landsat-8 Data. In: *IGARSS 2019–2019 IEEE International Geoscience and Remote Sensing Symposium*, pp. 7010–7013. <https://doi.org/10.1109/IGARSS.2019.8897798>.
- Laine, A.M., Korrensalo, A., Kokkonen, N.A.K., Tuittila, E.-S., 2021. Impact of long-term water level drawdown on functional plant trait composition of northern peatlands. *Funct. Ecol.* 35 (10), 2342–2357. <https://doi.org/10.1111/1365-2435.13883>.
- Larmola, T., Tuittila, E.-S., Tirola, M., Nykänen, H., Martikainen, P.J., Yrjölä, K., et al. Fritze, H., 2010. The role of Sphagnum mosses in the methane cycling of a boreal mire. *Ecology* 91 (8), 2356–2365. <https://doi.org/10.1890/09-1343.1>.
- Lee, G., Gommers, R., Waselewski, F., Wohlfahrt, K., O’Leary, A., 2019. PyWavelets: a Python package for wavelet analysis. *J. Open Source Softw.* 4 (36), 1237. <https://doi.org/10.21105/joss.01237>.
- Lees, K.J., Quaife, T., Artz, R.R.E., Khomik, M., Clark, J.M., 2018. Potential for using remote sensing to estimate carbon fluxes across northern peatlands – a review. *Sci. Total Environ.* 615, 857–874. <https://doi.org/10.1016/j.scitotenv.2017.09.103>.
- Lees, K.J., Artz, R.R.E., Khomik, M., Clark, J.M., Ritson, J., Hancock, M.H., Quaife, T., et al., 2020. Using spectral indices to estimate water content and GPP in Sphagnum Moss and Other peatland vegetation. *IEEE Trans. Geosci. Remote Sens.* 58 (7), 4547–4557. <https://doi.org/10.1109/TGRS.2019.2961479>.
- Lees, K.J., Artz, R.R.E., Chandler, D., Aspinall, T., Boulton, C.A., Buxton, J., Lenton, T.M., et al., 2021. Using remote sensing to assess peatland resilience by estimating soil surface moisture and drought recovery. *Sci. Total Environ.* 761, 143312 <https://doi.org/10.1016/j.scitotenv.2020.143312>.
- Lehnert, L.W., Meyer, H., Obermeier, W.A., Silva, B., Regeling, B., Bendix, J., 2019. Hyperspectral Data Analysis in R: The Hsdar Package. *J. Stat. Software* 89 (12), 1–23. <https://doi.org/10.18637/jss.v089.i12>.
- Letendre, J., Poulin, M., Rochefort, L., 2008. Sensitivity of spectral indices to CO₂ fluxes for several plant communities in a Sphagnum-dominated peatland. *Can. J. Remote. Sens.* 34 (sup2), S414–S425. <https://doi.org/10.5589/m08-053>.
- Li, D., Cheng, T., Yao, X., Zhang, Z., Tian, Y., Zhu, Y., Cao, W., 2016. Wavelet-based PROSPECT inversion for retrieving leaf mass per area (LMA) and equivalent water thickness (EWT) from leaf reflectance. In: *2016 IEEE International Geoscience and Remote Sensing Symposium (IGARSS)*, pp. 6910–6913. <https://doi.org/10.1109/IGARSS.2016.7730803>.
- Limpens, J., Berendse, F., Blodau, C., Canadell, J.G., Freeman, C., Holden, J., et al. Schaeppman-Strub, G., 2008. Peatlands and the carbon cycle: from local processes to global implications – a synthesis. *Biogeosciences* 5 (5), 1475–1491. <https://doi.org/10.5194/bg-5-1475-2008>.
- Lüdecke, D., Ben-Shachar, M., Patil, I., Waggoner, P., Makowski, D., 2021. Performance: An R Package for Assessment, Comparison and Testing of Statistical Models. *Journal of Open Source Software* 6 (60), 3139. <https://doi.org/10.21105/joss.03139>.
- Mallat, S.G., 1989. A theory for multiresolution signal decomposition: the wavelet representation. *IEEE Trans. Pattern Anal. Mach. Intell.* 11 (7), 674–693. <https://doi.org/10.1109/34.192463>.
- Meingast, K.M., Falkowski, M.J., Kane, E.S., Potvin, L.R., Benscoter, B.W., Smith, A.M.S., Miller, M.E., et al., 2014. Spectral detection of near-surface moisture content and water-table position in northern peatland ecosystems. *Remote Sens. Environ.* 152, 536–546. <https://doi.org/10.1016/j.rse.2014.07.014>.
- Mokhtari, A., Sadeghi, M., Afrasiabian, Y., Yu, K., 2023. OPTRAM-ET: a novel approach to remote sensing of actual evapotranspiration applied to Sentinel-2 and Landsat-8 observations. *Remote Sens. Environ.* 286, 113443 <https://doi.org/10.1016/j.rse.2022.113443>.
- Nelson, P.R., Maguire, A.J., Pierrat, Z., Orcutt, E.L., Yang, D., Serbin, S., Huemmrich, K. F., et al., 2022. Remote sensing of tundra ecosystems using high spectral resolution reflectance: opportunities and challenges. *J. Geophys. Res. Biogeosci.* 127 (2) <https://doi.org/10.1029/2021JG006697> e2021JG006697.
- Norouzi, S., Sadeghi, M., Tuller, M., Liaghat, A., Jones, S.B., Ebrahimian, H., 2022. A novel physical-empirical model linking shortwave infrared reflectance and soil water retention. *J. Hydrol.* 614, 128653 <https://doi.org/10.1016/j.jhydrol.2022.128653>.
- Olthof, I., Fraser, R.H., 2024. Mapping surface water dynamics (1985–2021) in the Hudson Bay lowlands, Canada using sub-pixel Landsat analysis. *Remote Sens. Environ.* 300, 113895 <https://doi.org/10.1016/j.rse.2023.113895>.
- Pan, Y., Birdsey, R.A., Fang, J., Houghton, R., Kauppi, P.E., Kurz, W.A., Hayes, D., et al., 2011. A large and persistent carbon sink in the World’s forests. *Science* 333 (6045), 988–993. <https://doi.org/10.1126/science.1201609>.
- Peñuelas, J., Pinol, J., Ogaya, R., Filella, I., 1997. Estimation of plant water concentration by the reflectance water index WI (R900/R970). *Int. J. Remote Sens.* 18 (13), 2869–2875. <https://doi.org/10.1080/014311697217396>.
- Räsänen, A., Tolvanen, A., Kareksela, S., 2022. Monitoring peatland water table depth with optical and radar satellite imagery. *Int. J. Appl. Earth Obs. Geoinf.* 112, 102866 <https://doi.org/10.1016/j.jag.2022.102866>.
- Rice, S.K., Aclander, L., Hanson, D.T., 2008. Do bryophyte shoot systems function like vascular plant leaves or canopies? Functional trait relationships in Sphagnum mosses (Sphagnaceae). *Am. J. Bot.* 95 (11), 1366–1374. <https://doi.org/10.3732/ajb.0800019>.
- Robroek, B.J.M., Schouten, M.G.C., Limpens, J., Berendse, F., Poorter, H., 2009. Interactive effects of water table and precipitation on net CO₂ assimilation of three CO-occurring Sphagnum mosses differing in distribution above the water table. *Glob. Chang. Biol.* 15 (3), 680–691. <https://doi.org/10.1111/j.1365-2486.2008.01724.x>.
- Rollin, E.M., Milton, E.J., 1998. Processing of high spectral resolution reflectance data for the retrieval of canopy water content information. *Remote Sens. Environ.* 65 (1), 86–92. [https://doi.org/10.1016/S0034-4257\(98\)00013-3](https://doi.org/10.1016/S0034-4257(98)00013-3).
- Rydin, H., Jeglum, J.K., 2006. *Biology of Peatlands*. Oxford University Press, Oxford, United Kingdom. <http://ebookcentral.proquest.com/lib/aalto-ebooks/detail.action?docID=430479>.
- Sadeghi, M., Jones, S.B., Philpot, W.D., 2015. A linear physically-based model for remote sensing of soil moisture using short wave infrared bands. *Remote Sens. Environ.* 164, 66–76. <https://doi.org/10.1016/j.rse.2015.04.007>.
- Sadeghi, M., Babaieian, E., Tuller, M., Jones, S.B., 2017. The optical trapezoid model: a novel approach to remote sensing of soil moisture applied to Sentinel-2 and Landsat-8 observations. *Remote Sens. Environ.* 198 (1), 52–69. <https://doi.org/10.1016/j.rse.2017.05.041>.
- Salko, S.-S., Juola, J., Burdun, I., Vasander, H., Rautiainen, M., 2023a. Intra- and interspecific variation in spectral properties of dominant Sphagnum moss species in boreal peatlands. *Ecol. Evol.* 13 (6), e10197 <https://doi.org/10.1002/ece3.10197>.
- Salko, S.-S., Juola, J., Burdun, I., Vasander, H., Rautiainen, M., 2023b. Reflectance spectra of nine boreal Sphagnum moss species. *Mendeley Data 1*. <https://doi.org/10.17632/WMSFXDMZD.1>.
- Schaeppman-Strub, G., Schaeppman, M.E., Painter, T.H., Dangel, S., Martonchik, J.V., 2006. Reflectance quantities in optical remote sensing—definitions and case studies. *Remote Sens. Environ.* 103 (1), 27–42. <https://doi.org/10.1016/j.rse.2006.03.002>.
- Tian, J., Zhu, X., Wu, J., Shen, M., Chen, J., 2020. Coarse-resolution satellite images overestimate urbanization effects on vegetation spring phenology. *Remote Sens.* 12 (1), 117. <https://doi.org/10.3390/rs12010117>.
- UNEP, 2022. *Global Peatlands Assessment – The State of the World’s Peatlands: Evidence for Action toward the Conservation, Restoration, and Sustainable Management of Peatlands*. Main Report. Global Peatlands Initiative. United Nations Environment Programme, Nairobi. <https://doi.org/10.59117/20.500.11822/41222>.
- Van Gaalen, K.E., Flanagan, L.B., Peddle, D.R., 2007. Photosynthesis, chlorophyll fluorescence and spectral reflectance in Sphagnum moss at varying water contents. *Oecologia* 153 (1), 19–28. <https://doi.org/10.1007/s00442-007-0718-y>.
- Verhoeven, J.T.A., Liefveld, W.M., 1997. The ecological significance of organochemical compounds in Sphagnum. *Acta Botanica Neerlandica* 46 (2), 117–130. <https://doi.org/10.1111/plb.1997.46.2.117>.

- Virtanen, P., Gommers, R., Oliphant, T.E., Haberland, M., Reddy, T., Cournapeau, D., SciPy, C., et al., 2020. SciPy 1.0: fundamental algorithms for scientific computing in Python. *Nat. Methods* 17, (3), 261–272. <https://doi.org/10.1038/s41592-019-0686-2>.
- Vogelmann, J.E., Rock, B.N., 1986. Assessing forest decline in coniferous forests of Vermont using NS-001 thematic mapper simulator data. *Int. J. Remote Sens.* 7 (10), 1303–1321. <https://doi.org/10.1080/01431168608948932>.
- Wang, L., Qu, J.J., 2007. NMDI: a normalized multi-band drought index for monitoring soil and vegetation moisture with satellite remote sensing. *Geophys. Res. Lett.* 34 (20) <https://doi.org/10.1029/2007GL031021>.
- Yu, Z., Loisel, J., Brosseau, D.P., Beilman, D.W., Hunt, S.J., 2010. Global peatland dynamics since the last glacial maximum. *Geophys. Res. Lett.* 37, (13) <https://doi.org/10.1029/2010GL043584>.
- Zhang, H., Väiliranta, M., Swindles, G.T., Aquino-López, M.A., Mullan, D., Tan, N., Zhao, Y., et al., 2022. Recent climate change has driven divergent hydrological shifts in high-latitude peatlands. *Nat. Commun.* 13 (1), 4959. <https://doi.org/10.1038/s41467-022-32711-4>.